EFFECT OF GEOMETRY ON THE PERFORMANCE OF MEMS ALUMINUM NITRIDE TRAMPOLINE RESONATORS IN LONGITUDINAL RESONANCE

Annie Ruimi [a], Yueming Liang [b] and Robert M. McMeeking [c]

[a] Texas A&M University at Qatar, Department of Mechanical Engineering
Doha, Qatar (annie.ruimi@qatar.tamu.edu)
[b] Exxon Mobil, Houston, TX, USA (yueming_liang@yahoo.com)
[c] University of California at Santa Barbara, Department of Mechanical Engineering,
Materials Department, CA, USA (rmcm@engineering.ucsb.edu)

ABSTRACT

The performance of a MEMS aluminum nitride trampoline-shape piezoelectric resonator is analyzed using three-dimensional finite element simulations. The device, targeted to operate at frequencies in the 3 GHz range is suitable for ultra-high-frequency (UHF) filtering applications. Material damping is accounted for in the model. The simulations are used to predict the effects of various geometric parameters on the resonator overall performance which is evaluated with the effective acoustic coupling coefficient (K^2) and the quality factor (Q) and extracted from the electrical impedance frequency response plots. The results indicate that (i) K^2 is insensitive to geometry (K^2~6.5%), (ii) Q increases linearly with the AlN thickness and (iii) a trampoline resonator with three legs is slightly more efficient than those with more.

1. INTRODUCTION

In the last ten years, there have been multiple research efforts to incorporate innovative microfabrication and material processing techniques to enhance the performance of resonators used in filters in the ultra-high-frequency (UHF) regime such as those required in wireless communication devices [1]-[8]. As a result, functioning microelectromechanical systems (MEMS)-based filter components with designs of various level of complexity have been built. Among them is a 3x3 array of trampoline-shape resonators fabricated at the University of California at Santa Barbara (UCSB) [9]. The device is shown in Fig. 1. It consists of nine circular resonator 300 μm in diameter, about 2 μm thick, supported by eight beams 300 μm long and 24 μm wide. The span between the resonators' centers is 1000 μm. The resonator and the beams are made of the piezoelectric material aluminum nitride chosen for its high acoustic velocity (~10927 m/s) and good piezoelectric coefficient (1.55 C/m2) [10]. The outer portion of each beam rests on a silicon substrate. The beams support the vibrating part of the structure and electrically connect the resonator via a MEMS component attached to the far ends of the beams. It is expected that the beams would minimize the transfer of acoustic energy from the resonating element to the surrounding system and diminish attachment loss that would result from clamping the membrane to the substrate. A gold electrode approximately 0.27 μm thick covers the top circular portion of the resonator so the beams are not piezoelectrically activated. The device is driven by a 1.5 GHz AC current oriented parallel to the axis of polarization (z-direction). By choosing an input frequency close to the natural frequency of the resonator, longitudinal (through-thickness) resonance is observed. For this particular type of MEMS applications, longitudinal over transverse vibrations are preferred because in the first instance, the resonant frequency varies as the inverse of the thickness according to the relation f=nV/2h (where n is the mode of vibration, h is the material's thickness and V is the material's acoustic velocity) while in the latter the resonant frequency are inversely proportional to the square of the length square. Consequently, attaining frequencies in the UHF regime, would require the difficult task to built resonators a few microns long while resonators a few microns thick would have the potential to attain frequencies in the order of GHz. In this case, the magnitude of the current takes into account the mass loading effects, i.e. the decrease of the resonance frequency due to the electrodes' added mass.

Fabrication techniques specific to the UCSB design can be found in [9]. They include an Inductively Coupled Plasma (ICP) chlorine process to etch the AlN and a MEMS-based bulk silicon Deep Reactive Ion Etch (DRIE) process to form a circular air cavity. The AlN film is sputtered directly onto a <100> silicon wafer. The UCSB Fabrication team has also characterized the performance of the device by measuring the electromechanical coupling coefficient K^2 and the quality Q-factor using a network analyzer. K^2 combines the elastic, piezoelectric and dielectric material coefficients [11] and is the ratio of electrical energy to mechanical energy stored in the device. A high value of K^2 is desired and associated with a broad bandwidth. The Q-factor measures mechanical losses and is an indication of the sharpness of the resonant response of the system. In theory, infinite values of Q can be achieved but in practice, values of Q on the order of only 10^3 are expected in this kind of electronic applications because filters have complex geometries and energy can dissipate at many locations [1]-[4]-[8].

Experimental values reported in [9] for the UCSB device include Q=150 and K^2=6.3% at 1.5 GHz which are significantly higher than those reported in the literature for similar designs [7] but the Q-s are not yet on the order of the expected thousand mentioned above, motivating further investigations. We have focused our efforts on developing three dimensional finite element models using the commercial FEM package Abaqus [12] to quantify the effects of various geometric parameters on the performance of the trampoline device. This is a systematic parametric study aimed at providing useful information to researchers at the design stages of piezoelectric resonators in view

978-1-4244-3481-7/09/$25.00 ©2009 IEEE

of the difficulties, length and cost associated with the reproduction in the lab of the various configurations we investigate.

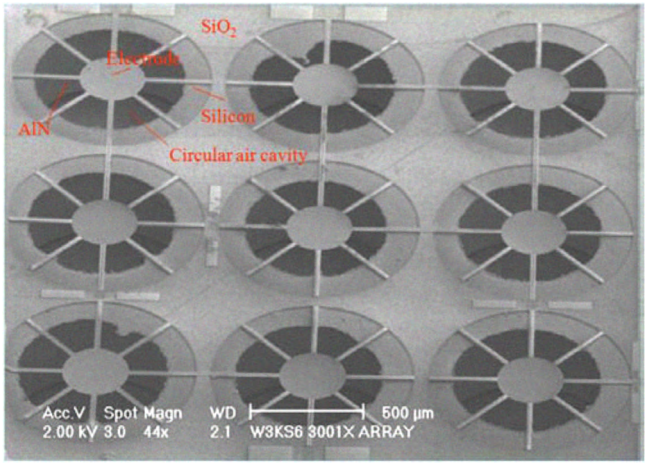

Figure 1. *3x3 Array of AlN trampoline resonators fabricated at UCSB.*

Our simulations use an eight-node, three-dimensional piezoelectric brick element (C3D8E) with four degrees of freedom per node, corresponding to three components of displacement and one electrical potential. The methodology we employ for the simulations is summarized as follows: Phase I investigates the performance of an ideal trampoline resonator where the electrodes thicknesses have been neglected and which is subjected to various changes in dimensions and geometry. Then, the resonator which has achieved the best performance values is assembled in pairs and quads to model a filter array (Phase II). The third phase consists in adding the electrodes to the resonator modeling. This has been described in [13]. Phase IV contains a more complete analysis of the resonator with electrodes encased in a silicon substrate. In the present paper, we report the results of Phase I.

2. THEORY

The relevant equations for lossless piezoelectric materials, assuming constant temperature, are

$$\begin{aligned} \{\mathbf{T}\} &= [\mathbf{C}^{\mathbf{E}}]\{\mathbf{S}\} - [\mathbf{e}]^{\mathbf{T}}\{\mathbf{E}\} \\ \{\mathbf{D}\} &= [\mathbf{e}]\{\mathbf{S}\} + [\boldsymbol{\varepsilon}^{\mathbf{S}}]\{\mathbf{E}\}, \end{aligned} \tag{1}$$

where **{T}**, **{S}**, **{E}** and **{D}** represent the stress, strain, electric field and electric displacement components respectively while $[\mathbf{c}^{\mathbf{E}}]$, $[\boldsymbol{\varepsilon}^{\mathbf{S}}]$ and **[e]** are the elasticity matrix at constant electric field, the dielectric permittivity matrix at constant strain and the matrix of piezoelectric coefficients [14]. The components of **E** are given by the gradient of the electric potential φ. The superscript T indicates the transpose.

A resonator behavior is characterized by its electrical impedance $Z(\omega)$, a complex quantity, defined as the ratio of voltage $V(\omega)$ over the current $I(\omega)$ and where ω is the natural frequency equal to 2πf. The performance values can be expressed as a combination of the resonant and anti-resonant frequencies that is the values that cause the impedance to be zero and infinite respectively [15]:

$$K^2 = \frac{\pi^2}{4}\left(\frac{f_a - f_r}{f_a}\right), \qquad Q_{r,a} = \frac{f_{r,a}}{2}\left|\frac{d\zeta}{df}\right|_{f_{r,a}} \tag{2}$$

K^2 is evaluated from the magnitude (real part) of the impedance while Q is evaluated from the phase angle (imaginary part) of the impedance. In 92), $|d\zeta/df|_{fr,a}$ is the absolute value of the derivative of the phase ζ evaluated at the resonant or the anti-resonant frequency.

In this work, we employ a particular form of damping known as Rayleigh damping which is written as a linear combination of the mass and stiffness matrix as **[C]=α[M] +β[K],** via two positive coefficients and which results in a set of uncoupled orthogonal modal equations of motion. The coefficient α is the mass proportional damping and simulates the process of a model moving through a viscous medium while the β coefficient can be thought as internal damping associated with the material itself [12]. In the simulations performed for this work, we assumed α to be zero and β was calculated to be equal to $2.82\text{x}10^{-14}$ s, a value slightly lower than the one reported in [16].

3. SIMULATIONS RESULTS

We simulated various configurations of aluminum nitride trampoline resonators enforcing the same mechanical and electrical boundary conditions as the device fabricated at UCSB as shown on Fig. 2. All external surfaces are stress free **(T=0)** except the ends of the beams which are fixed **(u=0)**. The surfaces for which no electrical potential is specified are charge free **(D.n=0)**. The bottom surface of the resonator has zero potential (φ =0) to represent a grounded electrode while the top surface is

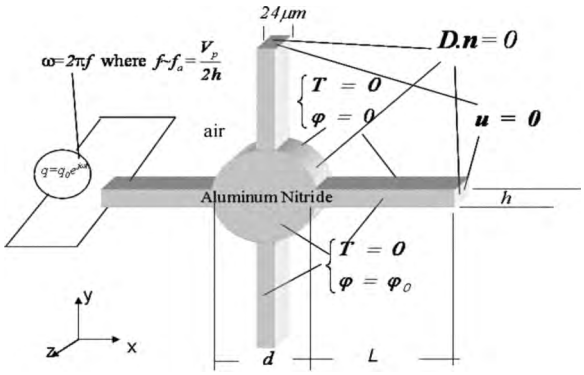

maintained at a uniform potential ($\varphi = \varphi_0$).

Figure 2. *Mechanical and electrical boundary conditions of the resonator enforced in the simulations.*

For each case, we generated the electrical impedance frequency response (EIFR) from which the resonant and anti-resonant frequencies were extracted. Then we calculated the the simulations refers to the geometry and dimensions of the resonator. The indices are the resonator's diameter, the number of legs, the legs length and the resonator thickness, respectively. For

instance d300-4l-100-1.7 refers to a trampoline resonator 300 µm in diameter, 1.7 µm thick, with four legs 100 µm long and 24 µm wide. The legs and the circular portion of the resonator have the same thickness. All simulations include a Rayleigh damping coefficient $\beta = 2.82 \times 10^{-14}$ s.

3.1 Through-Thickness Mode

Figure 3 shows the trampoline resonator 300 µm in diameter and 1.7 µm thick, with four legs 300 µm long and 24 µm wide, at rest and resonating in the thickness direction (-3 axis) at 3.17 GHz, a value reported by the Abaqus simulations (not legible on Fig. 3b). This value agrees very well with the one calculated from the EIFR plot generated from the simulation data and indicated on Fig. 3c by a sharp pick at 3.17 GHz. This value is also very close to 3.21 GHz which is the value obtained from a one-dimensional analysis using the relation $f_a = V/2h$. The small discrepancy is due to the fact that the simulations are three-dimensional and include damping. As expected, the damped system resonates at a frequency lower than the one that would result in an undamped system.

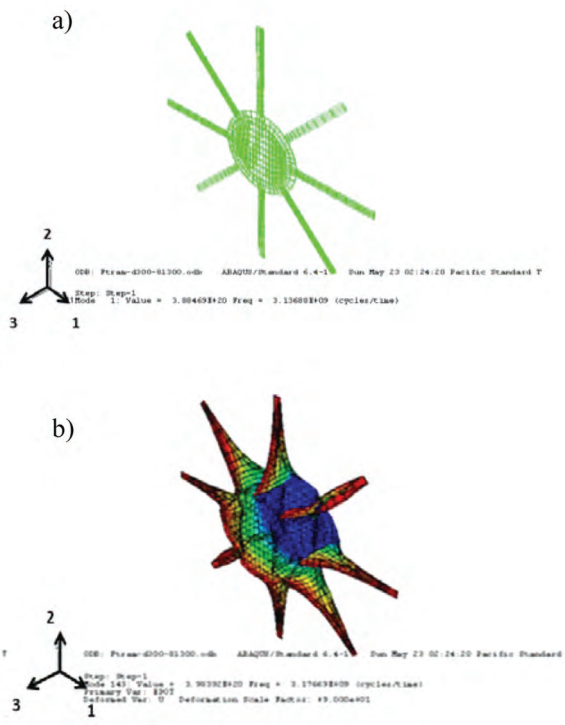

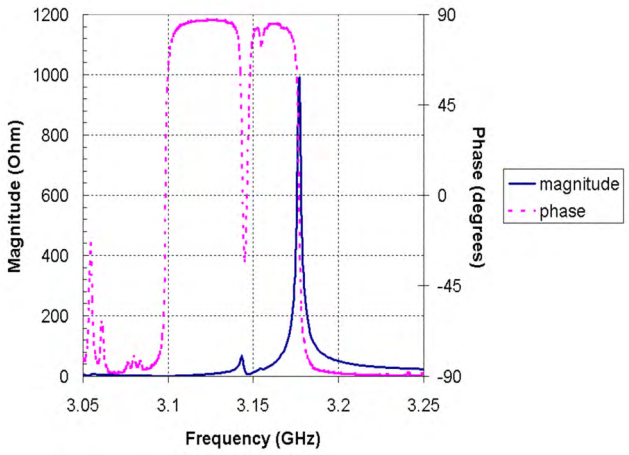

Figure 3. (a) *The AlN trampoline resonator d300-4l-300-1.7 at rest and (b) resonating at 3.17 GHz in a thickness-mode (3-direction). (c)EIFR generated from the FEM simulations showing a pick magnitude at 3.17 GHz.*

3.2 AlN Thickness

We performed six simulations of AlN trampoline resonators (d300-4l-100) with thicknesses ranging from 0.85 µm to 4 µm. Figure 4 shows the anti-resonant frequencies of the device as a function of the AlN thickness and how well they compare to those obtained from the one-dimensional undamped model. This is because, for a light damped system such as the one at hand, it can be shown that the resonant frequencies slightly differ from the ones obtained from the undamped model [17]. We plotted on Fig. 5 the performance coefficients obtain from (2) after generating the EIFR magnitude and phase plots for each thickness case. It shows that K^2 remains almost constant with thickness (K^2~6.15%), a value slightly higher than the one obtained with the one-dimensional undamped model (K^2=5.88%) but very close to the one measured for the UCSB device (6,3% [9]). The Q-factors range from 997 to 4475 and increase linearly with the AlN thickness. Furthermore, by substituting the estimated value of the anti-resonant frequency obtained from the one-dimensional model ($f_a = V/2h$) into the expression $Q_a = 1/\beta\omega_a$, the expression $Q_a = h/\pi V\beta$ is obtained. This simple model makes it clear that Q_a values are in fact proportional to the resonator's thickness. Thus, thick resonators are capable of achieving high values of Q however the magnitude of the anti-resonant frequency also drops significantly illustrating some of the trade-off associated with design decisions.

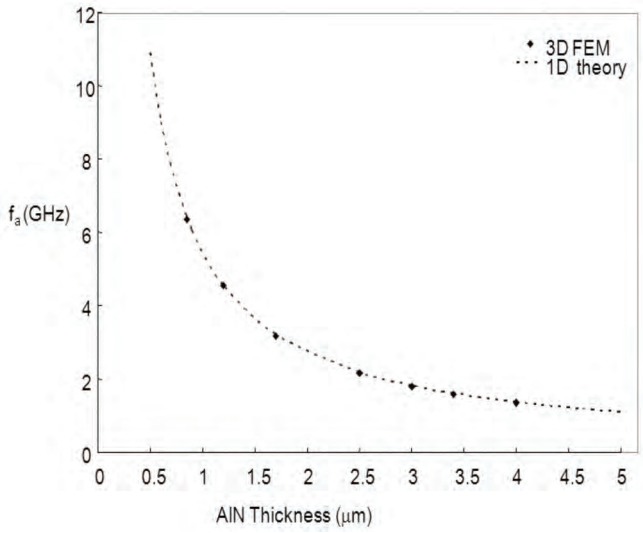

Figure 4. *Anti-resonant frequencies (f_a) as a function of AlN thickness. Results obtained from the simulations of d300-4l-100-** resonators.*

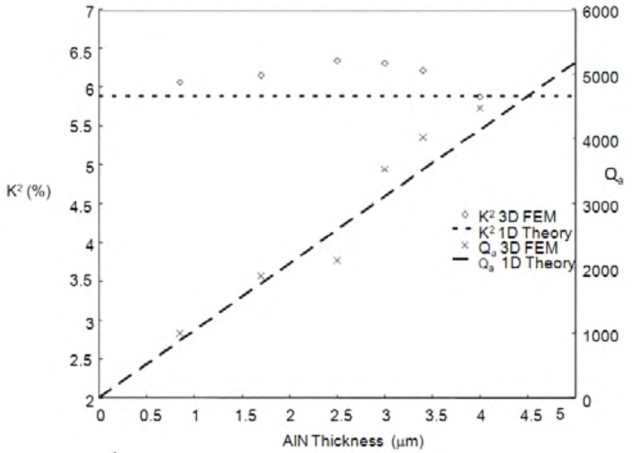

Figure 5. *K^2 (left axis) and Q-factor (right axis) as a function of AlN thickness. Results obtained from the simulations of d300-4l-100-** resonators.*

3.3 Leg Length

Figure 6 shows the EIFR obtained from the simulations of trampoline resonators (d300-8l-**-1.7) with leg length varying from 100 μm to 300 μm. There is an excitation of spurious modes between the resonant and anti-resonant frequencies which increases with the beam length. The performance values are summarized in Table I. It shows that the leg length has minimal effect on K^2 and Q. Most of the dissipated energy at resonance is lost in the central portion of the resonator so the added leg's length on the performance of the resonator is minimal. This had been confirmed by the values measured for the device fabricated at UCSB Fabrication [9]. However, Fig. 6 brings out clearly that as the leg length is increased, spurious modes become stronger and shift to the right and closer to the anti-resonance peak which will potentially affect the value of Q_a if the spurious modes approach the anti-resonant frequency too closely. On the other hand, the results suggest by extrapolation that if the beams are too short, the spurious modes would be in the proximity of the resonant frequency and would result in greater dissipation during resonance and a degraded Q-factor.

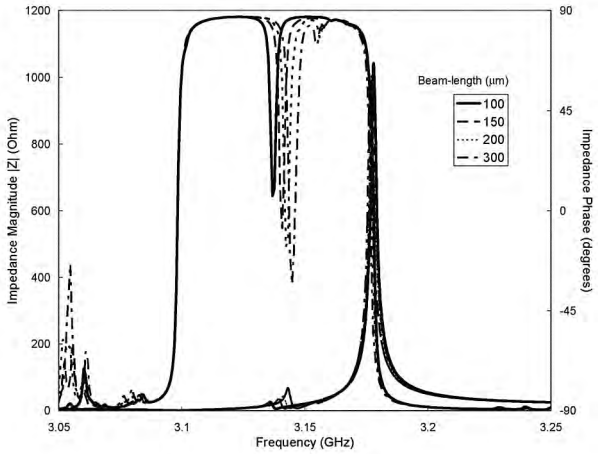

Figure 6. *Effect of leg length on the EIFR magnitude and phase. Results obtained from the simulations of d300-8l-**1.7 resonators.*

Table I. ***Performance coefficients as a function of leg length.***

Leg Length (μm)	K^2 (%)	Q_a
100	**6.15**	**1789**
150	**6.15**	**1730**
200	**6.09**	**1650**
300	**6.09**	**1786**

3.4 Number of Legs

We performed FEM simulations of a trampoline resonator 300 μm in diameter with three, four or eight legs, 100 μm long and 1.7 μm thick. Figure 7 shows how the number of legs affects the EIFR. The obvious feature is that the resonator with three legs experiences resonance and anti-resonance at about 20 MHz higher than the two others but the relative separation between the resonant and anti-resonant frequencies remains constant yielding K^2~6.1% and a Q~1800. The performance coefficients are summarized in Table II and show that the performance increases with a decreasing number of legs. An explanation for the behavior is that the three-beam resonator has the beams approximately aligned with the three principal crystallographic

directions of AlN (120^0 apart each), where material properties are identical and damping is minimal. Fewer beams apply less constraint or disturbance to the vibration modes of the center of the trampoline and tend to eliminate the rotational and/or radial component of the displacement. This results in a mode that is closer to the ideal pure longitudinal mode where the circular portion of the resonator expands only in the thickness direction and for which Q is the highest. We note that this is in contradiction to the lab measurements where the eight-leg resonator has yielded higher performance values [9].

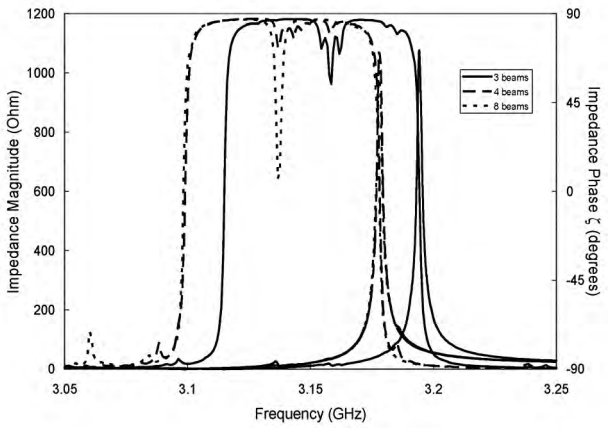

Figure 7. *Effect of the number of legs on the EIFR magnitude and phase. Results obtained from the simulations of d300-**-100-1.7 resonators.*

Table II. ***Performance coefficients as a function of number of legs.***

Number of legs	K^2 (%)	Q_a
3	**6.09**	**1950**
4	**6.09**	**1880**
8	**6.15**	**1789**

4. CONCLUSIONS

Three-dimensional finite element simulations were used to evaluate the effects of geometry on the performance of an aluminum nitride trampoline-shape resonator designed for filtering applications. The electrodes were assumed of negligible thickness but damping was accounted for in the simulations. The resonator was forced by a harmonically varying electrical current over a range of frequencies. The resonators thicknesses ranged between 0.85 μm to 4 μm to maximize the magnitude of the resonant frequency. Performance was evaluated by means of the effective acoustic coupling coefficient K^2 and the Q-factors which were calculated from the magnitude and phase of the electrical impedance frequency response (EIFR) plots. The values were compared to measurements obtained during the testing of a device of similar geometry fabricated at UCSB.

The results indicated that K^2 was constant (~6.0%) and insensitive to the resonator's thickness and leg length, ii) the resonator with three legs was slightly more efficient than the device with four or eight legs and iii) the Q- factors increased linearly with the device thickness and a Q on the order of 2000 was calculated for the resonator approximately 2 μm thick. The trends and results compared well with those obtained from a one-dimensional theory suggesting that key performance parameters of resonators could be evaluated from a simple one dimensional analysis. The main concern is the discrepancy between the values of Q obtained from the simulations and those measured in the lab which are about ten times lower. However it is timely to recall that we neglected the electrodes in these simulations and that they are well know mechanisms for energy dissipation.

ACKNOWLEDGMENTS

This work was supported in part by the Defense Advanced Research Project Agency ONR/MINT under contract N66001-01-1 8965. Figure 1 was reproduced with permission of N. C. Mac Donald et al. at UCSB [9].

5. REFERENCES

[1] Nguyen, C. T.–C., 1998, "Microelectromechanical devices for wireless communications," *Proceedings IEEE International Microelectromech. Syst. Workshop*, Heidelberg, Germany, Jan. 25-29, pp. 1-7.

[2] Bannon, F.D., III, Clark, J.R., Nguyen, C. T.-C, Apr. 2000, "High-Q high frequency micromechanical filters", *IEEE J. Solid-State Circuits*, **vol. 35**, pp. 512-526.

[3] Ruby, R. C. , Bradley, P. , Oshmyansky, Y. , Chien A., and Larson, J.D. III, 2001, "Thin film bulk wave acoustic resonators (FBAR) for wireless applications", *IEEE Ultrasonics Symposium*, Piscataway, NJ, pp. 813-821.

[4] Lakin, M., 2001, "Thin film resonators and high frequency filters, TFR Technologies, Inc.

[5] Antkowiak, B., Gorman, J.P., Varghese, Carter, D.J.D., Duwel, A.E., June 8-12, 2003, "Design of high-Q low-impedance, GHZ-range piezoelectric MEMS resonator", *12th Int. Conf. Solid State Sensors, Actuators and Microsystems*, Boston.

[6] Fattinger, G. G., Kaitila, J., Aigner, R. , Nesler, W. , 2003, "Thin film bulk acoustic wave devices for applications at 5.2 GHz", *IEEE Ultrasonics Symposium*, pp. 174 -177.

[7] Kim, H.H., Ju, B.K., Lee, Y. H., Lee, S.H., Lee, J.K., Kim, S.W., 2004, "Fabrication of suspended thin film resonator for application of RF bandpass filter", *Microelectronics Reliability,* **vol. 44**, pp. 237-243.

[8] Clark, J.R., Hsu, W., Abdelmoneum, A., Nguyen, C. T.-C., Dec. 2005, "High-Q UHF micromechanical radial-contour mode disk resonators", *J. Microelectromech. Syst*, **vol. 14,** pp. 1298-1310.

[9] Callaghan, L. A., Lughi, V., MacDonald, N. C., Clarke, D. R., 2006, "Beam-supported AlN thin film bulk acoustic resonators", *IEEE Trans. Ultrason. Ferroelect. Freq. Contr.*, **53**, pp. 1101-1007.

[10] Cleland, A.N., Pophristic, M., Ferguson, I., Sept. 2001, "Single-crystal aluminum nitride nanomechanical resonators," **vol. 79**, pp. 2070-2072.

[11] Rosenbaum, F., 1988, *Bulk Acoustic Wave Theory and Devices*, Arthech House, Boston, Chap.4-5-10.

[12] Abaqus Explicit/User's Manual, Version 6.4, Hibbitt, Karlson & Sorensen, Inc. 2003.

[13] Ruimi, A., Liang, Y., and McMeeking, R.M., Nov 2008, "UHF aluminum nitride FBAR trampoline-shape resonators with gold-aluminum electrodes and silicon substrate with through thickness vibrations: computational performance", *International Journal of Mathematics and Computation, Vol 1, Issue N08, Nov 2008.*

[14] Dieulesaint, E., Royer, D., 1980, *Elastic Waves in Solids*, John Willey & Sons, Chapt.7.

[15] Auld, B.A., 1990, *Acoustic Fields and Waves in Solids*, Volume I, 2nd ed. Krieger, Malabar, FL, Chapt. 8.

[16] Ballato, A., and Gualtieri, J. G., "Advances in high-Q piezoelectric resonator materials and devices," *IEEE Trans. Ultrason. Ferroelect. Freq. Contr.*, vol. 41, pp. 834-844, Nov. 1994.

[17] Yong, Y.Y. and Patel, M.S. "Piezoelectric resonators with mechanical damping and resistance in current conduction", *Science in China Series G: Physics, Mechanics and Astronomy*, vol.50, no. 5, pp. 650-672, Oct. 2007.